TEXTURE AND RESIDUAL STRAIN MEASUREMENTS ON POLISHED ALLOY 600 COUPONS CONTAINING TWO SCRATCHES USING SYNCHROTRON MICRO-LAUE DIFFRACTION

Marina Fuller, Sridhar Ramamurthy, Stewart McIntyre, Robert Klassen,
The University of Western Ontario
Peter King,
Babcock & Wilcox Canada
Andrea Gerson,
University of South Australia
Wenjun Liu,
Advanced Photon Source, Chicago

ABSTRACT

Mechanical strain fields near two mechanical scratches (40 and 2 μm deep respectively) on polished Alloy 600 surface have been studied using micro-Laue diffraction technique with the beamline 34-ID at the Advanced Photon Source (APS), Argonne, Illinois. Three-dimensional resolution of the diffraction patterns is enabled by differential aperture X-ray microscopy (DAXM). The DAXM technique is capable of producing depth resolved local grain orientation and strain distribution maps. The material under the deep scratch was found to be severely deformed in the entire sampling depth: i.e., only a diffuse Laue pattern was observed. Grain structure was detected at regions away from the scratch to depths of 60 to 100 μm into the metal. In contrast, a three layered structure was observed for the material under the shallow scratch: a nanocrystalline layer to a depth of 20 μm (diffuse Laue pattern), followed by a plastically deformed region (streaked Laue pattern) of approximately 10 μm in depth, and then a slightly deformed grain structure (indexed Laue patterns). The residual strain distribution maps indicate that the strain under the shallow scratch region appears to be triaxial.

This is the first major study where three-dimensional grain orientation and strain mapping has been applied to the study of nickel-based steam generator tubing materials. The ability to produce micro-strain distribution laterally and depth wise across several grains would be very useful in enhancing the understanding the stress corrosion cracking behaviour of these alloys. Laboratory simulations tend to suggest that under certain operating conditions, stress corrosion cracking (SCC) could occur at locations that have sustained mechanical damage such as dings, dent and fret marks during manufacturing and/or operation. If micro-strain distribution at deformed regions can be determined under these conditions, then it is potentially possible to determine the critical strain level(s) that could result in crack initiation.

1.0 INTRODUCTION

Stress corrosion cracking (SCC) is an active degradation mechanism in both CANDU (CANada Deuterium Uranium) heavy water and PWR (pressure water reactor) light water steam generators (SGs) [1-8]. Alloy 600, a nickel-rich alloy, has been used as the primary SG material in some of the reactors in the CANDU fleet and has been found to fail by SCC [5,8]. This alloy is being replaced by Alloy 800 in CANDU reactors and by Alloy 690 in light water reactors. While these alloys have known to be more resistant to SCC compared to Alloy 600, it is also recognized that SCC can occur under certain conditions and that certain locations that have sustained mechanical damage (such as fretting, dings and dent marks) during manufacturing and/or operation are potential initiation sites [9-11].

To improve the prediction of the onset of cracking under these conditions requires that the interplay of mechanical and chemical behaviour of this material be thoroughly understood. The effects of chemical environments on SCC in nickel alloys are known to a certain degree [5-7,11,12]; however, the effects on mechanical stress on a microscopic scale are less well understood. Their combined effects therefore have not been well characterized. Micro-strain measurement by Laue X-ray diffraction is a relatively new technique that appears to be capable of determining the distribution of strain intensity and its direction in polycrystalline alloys [13-16]. This technique has recently been used to study the local grain orientation and residual stress in polished Alloy 600 coupons subjected to mechanical stresses similar to steam generator regimes. Our initial studies involved the analyses of two scratches, one ‘coarse’ and one ‘fine’, on the surfaces of A600 coupons and the results from these measurements along with the description of the Laue technique are presented in this paper.

2.0 LAUE DIFFRACTION TECHNIQUE FOR MICROSTRAIN MEASUREMENTS

2.1 Advantages of Laue Diffraction

Synchrotron based micro Laue diffraction enables the depth resolved measurement of crystal orientation and stress/strain. Mechanical measurements of stress result in the destruction of the item being examined and hence, repeat or further analyses are not possible. X-ray (and neutron) diffraction based measurements offer a non-destructive method of evaluating residual stress in materials. The residual stress is calculated assuming a linear elastic distortion of the crystal lattice.

X-ray penetration into steel samples using a traditional laboratory based X-ray generator is generally rather shallow, < 10 μm, and hence the stress is described by two principal components, orientated perpendicular to each other within the plane of the surface. A polychromatic, high energy X-ray beam, as supplied by a synchrotron, results in greater penetration into the sample than obtainable using a laboratory based X-ray source. The depth of penetration of a high energy synchrotron X-ray source enables the full stress tensor, including the components perpendicular to the surface, to be determined. In addition, by using a polychromatic X-ray source, the Bragg condition can be fulfilled for several Miller indices simultaneously. In this manner, sufficient diffraction data can be collected from many

crystalline grains simultaneously, without the need to rotate either the sample or the detector. Synchrotron microdiffraction provides the only practical non-destructive means by which to carry out 3D crystallographic orientation and strain mapping.

2.2 Beamline 34ID at the Advanced Photon Source (APS), Argonne National Laboratory

In order to be able to carry out diffraction mapping in 3D to a reasonable penetration depth and resolution the following X-ray characteristics are required:
1) polychromatic, high energy incident X-rays (8-20 keV)
2) small spot size (~ 1 μm x 1 μm)
3) low divergence
4) high incident flux while satisfying 1) to 3)

These requirements are most adequately fulfilled by beamline 34-ID-E at the Advanced Photon Source (APS), Argonne National Laboratory, Argonne, Illinois. A schematic of the layout of the end-station is shown in Figure 1. The monochromator is constructed in such a way that on lateral translation, either a white (polychromatic) beam or monochromatic beam is incident on the sample. The beam is then focussed by a KB mirror pair and is incident on the sample at an angle of approximately 45°. The diffraction patterns are measured on a CCD camera placed above the sample. The sample is imaged by moving the sample either laterally or vertically.

2.3 3D Laue Measurements: Differential Aperture X-ray Microscopy (DAXM)

Resolution of the diffraction patterns in 3D is enabled by differential aperture X-ray microscopy (DAXM). This entails scanning an extremely thin (50 microns in diameter) wire using micron size steps, across the face of the sample so that diffraction spots on the CCD camera are systematically extinguished. It is then possible, by tracing back from the CCD camera to the position of the wire, and to the incident x-ray beam path, to establish from what depth a diffraction spot originated from. A computer program developed previously [13,17] collates and reconstructs the full Laue diffraction images from micron or submicron (depending on hardware parameters) voxels along the penetration depth of the synchrotron X-ray beam (see Figure 2). The reconstructed Laue images are then analysed using previously developed computer indexing, crystallographic orientation and stress/strain tensor analyses [13,17].

3.0 EXPERIMENTAL METHODOLOGY

3.1 Sample Preparation

Flat Alloy 600 coupons (2.5 cm x 1.25 cm x 0.6 cm thick) were procured from Metal Samples in the annealed condition. The bulk composition (wt.%) of this is as follows: 0.050%C, 14.8%Cr, 77.9%Ni and 6.29% Fe. One face of these coupons was polished to 1 μm surface finish using diamond paste. Then, two approximately 100 μm wide scratches were made on the polished surface along the length of the coupons. A micrometer tip was used for this purpose so that the

scratches of consistent depth and width could be generated on all coupons. Figure 3 presents an optical micrograph of the Alloy 600 containing one such scratch. In this figure, the scratch is at the far right and the adjacent areas have been etched to reveal the grain structure. Close examination of the edge of the scratch indicates the presence of slip planes generated from the scratching process. The figure on the right presents a surface profile across the scratch generated using a Profilometer. This surface scan indicates that the scratch is approximately 100 μm wide and 40 μm deep. Due to the nature of the scratch generated by this methodology, this scratch has been identified as a 'coarse' scratch. This surface scan also indicates the pile-up at the edges of the scratch.

In addition to the coarse scratch, a thin and fine scratch was also generated on another polished Alloy 600 coupon surface using the following methodology. An Alloy 600 coupon surface was polished to 0.5 μm surface finish using a silica colloidal solution. The polished surface was then etched by immersion in a Glyceragia solution (10 ml NHO_3, 25 ml HCl, 30 ml Glycerin) for 90 seconds. A scratch of approximately 1500 μm in length was made using a spherical diamond tipped nano indenter. The geometry of the tip was similar to that of a Brinell indenter. A constant load of 400 mN with an indenter tip velocity of 1 μm/s was used to generate the scratches. Figure 4 shows the optical micrograph of this scratch (left figure) and the scratch is at the far left of this figure. The slip lines emanating from the edge of the scratch can also be seen in this figure and the red line indicates the region up to which the slip planes extend across the metal surface. The figure on the right is a surface profile of this scratch and indicates that the scratch is approximately 20 μm wide and 1.5 μm deep. Pile up of material at the edge of the scratch can also be seen in this figure.

3.2 Examination of Scratched Coupons Using Laue Diffraction

Microdiffraction data was collected on the UNICAT ID-34-E Microdiffraction beamline at the Advanced Photon Source, Argonne, IL. The metal coupon was placed in the beamline at an angle of approximately 45° with respect to the incident X-ray micro beam. A polychromatic synchrotron X-ray micro beam, focussed to approximately 0.5 μm in diameter by elliptically configured K-B mirrors, was used for the measurements. For the depth resolved Differential aperture X-ray microscopy (DAXM) measurements, a platinum wire profiler, approximately 50 μm in thickness, was used. The DAXM measurements involved stepping the wire profiler across surface of the sample in one micron steps and collecting a CCD image at each wire position. For these experiments, the wire was moved over a distance of 399 μm, resulting in the collection of 400 CCD images at each incident synchrotron x-ray beam position on the sample. The depth resolution is approximately one micron and lateral resolution for these measurements is one micron. Previously developed software was used to collate and then reconstruct the full Laue images with one micron resolution along the penetration direction of the synchrotron x-ray beam (Figure 2). The reconstructed Laue images were then analysed using previously developed computer indexing, crystallographic orientation and stress/strain tensor analyses.

4.0 RESULTS AND DISCUSSION

4.1 Laue Microdiffraction Data from the Coarse Scratch Sample

Figure 3 shows the optical micrograph of the etched surface near the coarse scratch region. This figure shows that the grain size varied anywhere from approximately 15 μm to 200 μm. Moreover, slip planes extending approximately 100 to 150 μm from the scratch edge can also be seen in this figure. On this sample, an area of approximately 200 μm x 50 μm was analysed by micro Laue diffraction, covering part of the scratch region and extending approximately 150 μm away from the scratch region. A step size of one μm was used for the mapping. As a first step, DAXM technique was not used for data collection; this enables us to obtain two-dimensional orientation maps of the grain structure within the analysis area. The resulting two-dimensional grain orientation map for the [1,1,1] crystallographic direction, along with a telescope image of the sample area are presented in Figure 5. The Laue diffraction pattern from the grains to the left of the scratch can be indexed and hence their orientation information is presented in this figure. However, the area within the scratch did not get indexed due to the significant deformation sustained in this region and hence its orientation appears to be black in this figure. Finally, the optical micrograph in Figure 3, the telescopic image and the orientation map in Figure 5 indicate that the area near the edge of the scratch also appears to be deformed.

Representative CCD images of the Laue diffraction pattern from three selected areas are presented in Figure 6a-c. These areas correspond to the locations A, B and C shown in Figure 5. The CCD image taken furthest away from the scratch region (A) shows some moderate streaking of the Laue spots, thus indicating some deformation. As the scratch region is approached, the diffraction spots become progressively streaked as shown in area B. The CCD images from area C (scratch region) show only diffuse structure, thus indicating that the grain structure under the scratch has been disrupted to the extent that the material is now nanocrystalline. It should also be mentioned that the CCD images that show severely streaked patterns and those showing only diffuse structure did not get indexed (crystal orientation not determined) and hence appear as black areas in the OM. Hughes and Hansen [18] reported that nanostructured copper can be produced by deformation under large sliding loads. 10 nm scale microstructures were formed in the near surface and coarsen with increasing depth.

Figures 5 and 6 show that the extent of the deformation in and around the scratch region can be qualitatively determined from Laue diffraction patterns. For example, the extent of streaking appears to provide direct correlation to the extent of plastic deformation. Even though this qualitative information can be very useful, one of the major advantages of this technique is the ability to produce depth-resolved strain formation. This has been illustrated using the data from the fine scratch sample.

4.2 Laue Microdiffraction Data from the Fine Scratch Sample

The optical micrograph highlighting an edge of the fine scratch is shown in Figure 4. The region between the edge of the scratch on the left and the red line on the right exhibits light coloured slip planes resulting from the plastic deformation due to scratching. The width of the plastically deformed region extrapolated across both edges of the scratch appears to be of the order of 30 μm.

Laue diffraction data was collected using the depth resolved differential aperture X-ray microscopy (DAXM) technique along a 50 μm long line scan across the fine scratch. The synchrotron beam step size was 1 μm, which enabled us to collect 51 data points along this line. The resulting orientation map for the [1,1,1] crystallographic direction and the representative depth integrated and depth resolved (reconstructed) CCD images of Laue diffraction pattern are presented in Figure 7. The solid blue line across the top of the orientation map indicates the sample surface, above which the reconstructed CCD images were found to be devoid of any structure. Note that the reconstruction process generates CCD images for a user defined distance along the synchrotron incident x-ray beam path through air and the sample. CCD images between the solid blue and green lines were found to exhibit diffuse structure (no defined Laue spots) as shown in CCD image (a), corresponding to that from position 'a' in the orientation map. The CCD image (b) from the grain labelled 'b' in the orientation map exhibits well-defined round spots. On the other hand, the CCD images (c) and (d) from positions 'c' and 'd' in the orientation map exhibit severe streaking towards the top right corner of the CCD image. These CCD images are believed to originate from the side of the scratch. The CCD image (e) from position 'e' in the orientation map also exhibits streaking, however, the streaking is more vertical than that seen in (c) and (d). The direction of the Laue pattern streaking is indicative of crystal rotation direction in the context of the laboratory reference frame. The streaks in images (c), (d) and (e) are in approximately the same positions as those from the indexed grain 'b' indicating that the material in these regions is related to grain 'b' but has been plastically deformed.

This figure also indicates the presence of a plastically deformed area in the orientation map (black area which was not indexed), of approximately 30 μm x 30 μm in size. This corresponds approximately to the width of the slip planes (plastic zone) extrapolated from the optical image shown in Figure 4.

Reconstructed (depth resolved) CCD images from the fine scratch from the position marked by the purple line in the OM shown in Figure 7 (scratch edge), are presented in Figure 8. The approximate sample depth (relative to the surface) is indicated in microns above the reconstructed CCD images and streaks in the regions indicated by the black box are blown up below the respective CCD images for comparison. Laue diffraction images from measurements using synchrotron x-ray microbeams have been shown to be sensitive to the hierarchical distribution of dislocations and can be used to study the orientation and density of individual geometrically necessary dislocations (GNDs) and geometrically necessary boundaries (GNBs) [15, 19]. The blown up streak from the 8 micron depth shows splitting of the streak indicating the formation of GNBs separated by cells rotated by the deformation and individual GNDs. Splitting is still evident in the image from the 13 micron depth and the streaking has moved towards the upper right indicating rotation of cells. These reconstructed Laue images represent one micron volumes within the sample and show the plastic response of the material to mechanical scratching. The streaked Laue images from the 8 and 13 microns depths are related to the grain represented by the Laue image at 18 microns.

Figure 9 shows the ϵ_{xx}, ϵ_{yy} and ϵ_{zz} deviatoric strain component maps corresponding to the orientation map for the [1,1,1] crystallographic direction collected from the fine scratch sample (also shown in Figure 7). The strain values are in 10^{-3} units and a thermal scale has been

employed to show the distribution of tensile and compressive strains within the analysis area. Coordinates of sample orientation matrix in indexed files are as follows: y-direction is in the direction of the generated scratch, x-direction runs perpendicular to the scratch direction and the z-direction is perpendicular to the sample surface (i.e., the DAXM line scan was taken perpendicular to the scratch). The regions marked A-C in the ϵ_{xx} strain component map correspond roughly to the grain structure in the corresponding OM. The grains on either side of grain B (A and C) are in different states of strain, A being compressive and C tensile. The grains under the scratch show triaxial strain.

5. CONCLUSIONS

Preliminary Laue diffraction measurements were performed on two polished Alloy 600 samples. One contained a coarse scratch of approximately 100 μm wide and 40 μm deep, while the other contained a fine scratch of approximately 20 μm wide and 1.5 μm deep. Laue diffraction measurements were performed along a line across the scratch starting from the scratch region. The results indicate that:

(1) The material under the coarse scratch was found to be severely deformed (nanocrystalline), at least to the sampling depth of the technique - i.e., only diffuse structure was observed in the CCD images from this region.

(2) A layered structure was observed for the material under the 'fine' scratch with a nanocrystalline layer extending down approximately 20 μm under the scratch, followed by a plastically deformed region (streaked Laue pattern) of approximately 10 microns in depth, and then finally, intact grain structure (indexed Laue patterns).

(3) The area of the plastic zone determined from Laue diffraction patterns (i.e. the area not indexed) was approximately 30 μm x 30 μm in size. This reasonably corresponds to the width of the slip planes observed using optical microscopy.

(4) The versatility of this technique and the ability to produce depth-resolved strain information makes this technique quite useful for the verification of data from theoretical modelling.

6. ACKNOWLEDGEMENTS

The authors would like to acknowledge the funding contributions from Babcock & Wilcox Canada (BWC) and the Centre for Materials and Manufacturing Ontario (CMM). We would also like to thank Mr. H. Wang, Department of Materials Engineering, University of Western Ontario, for the metallographic sample preparation and Mr. Peter King of BWC and Mr. Edward Lehockey of Ontario Power Generation for many useful discussions. Use of the Advanced Photon Source (APS) was supported by the U.S. Department of Energy, Office of Science,

Office of Basic Energy Sciences, under Contract No. W-31-109-ENG-38. Permission from Beamline 34ID for the use of Figures 1 and 2 is also acknowledged.

7. REFERENCES

1. R. Kilian and A. Roth, Materials and Corrosion, 53, 2002, pp. 727-739
2. P. Berge, Materials Performance, 36, 1997, pp. 56-62.
3. K. Gott, Key Engineering Materials, 261-263, 2004, pp. 845-854.
4. S.D. Strauss, Power, 140, 1996, pp. 29-30.
5. P.M. Scott, Corrosion, 56, 2000, pp. 771-782.
6. L.E. Thomas and S.M. Bruemmer, Corrosion, 56, 2000, pp. 572-587.
7. R.L. Tapping, J. Nickerson, P. Spekkens and C. Maruska, Nuclear Engineering and Design, 197, 2000, pp. 213-223.
8. G.S. Was, Corrosion, 46 1990, p. 319.\
9. W. Yang, Z. Lu, D. Huang, D. Kong, G. Zhao and J. Congleton, Corrosion Science, 43, 2001, pp. 963-977.
10. F. Vaillant, D. Buisine and B. Prieux, Proc. Seventh International Symposium on Environmental Degradation of Materials in Nuclear Power Systems--Water Reactors. Vol. I; Breckenridge, CO; USA; 1995, pp. 219-231.
11. C.M. Owens, Materials Performance, 25, 1986, pp. 49-54.
12. T.J. Marrow, L. Babout, A.P. Jikov, P. Wood, D. Engelberg, N., Stevens. P.J. Withers and R.C. Newman, J. Nuclear Materials, 352, 2006, pp. 62-74.
13. G.E. Ice and B.C. Larson, Adv. Eng. Mater. 2, 2000, pp. 643-646.
14. B.C. Larson, Wenge Yang, G.E. Ice, J.D. Budai and J.Z. Tischler, Nature 415, 2002, pp. 887-890.
15. R.I. Barabash and G.E. Ice, *Encylopedia of Materials: Science and Technology Updates*, Elsevier Press, 2005, pp. 1-18.
16. G.E. Ice, B.C. Larson, J.Z. Tischler, W. Liu and W. Yang, Materials Science and Engineering, 399, 2005, pp. 43-48.
17. J.-S. Chung and G.E. Ice, J. Appl. Phys. 86, 1999, pp. 5249-5255.
18. D.A. Hughes and N. Hansen, Phys. Rev. Lett. 87, 2001, pp.135503-1 – 135503-4.
19. R.I. Barabash, G.E. Ice, B.C. Larson and W. Yang, Rev. Sci. Instrum., 73, 2002, pp.1652-1654.

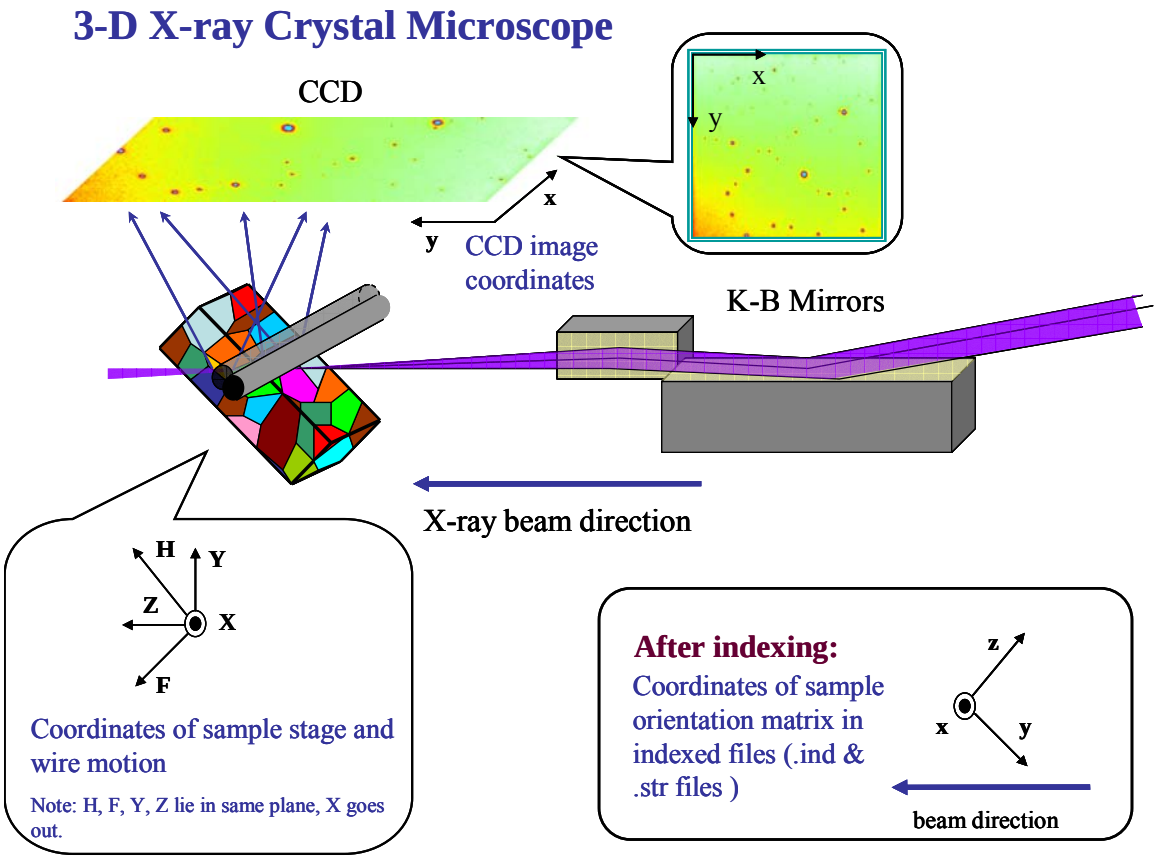

Figure 1. A schematic of the layout of the end-station at the 34-ID-E beamline at the Advanced Photon Source (APS), Argonne National Laboratory, Argonne, Illinois

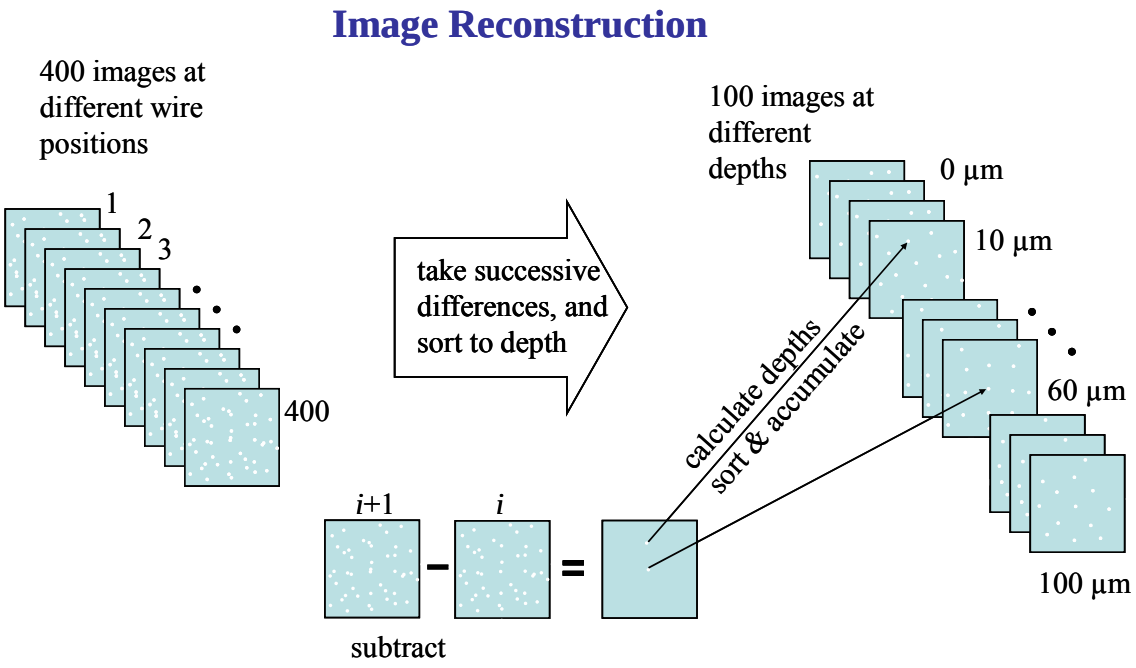

Figure 2. Image reconstruction process employed for processing Laue diffraction data. This process collates and reconstructs the full Laue diffraction images from micron or submicron (depending on hardware parameters) voxels along the penetration depth of the synchrotron X-ray beam.

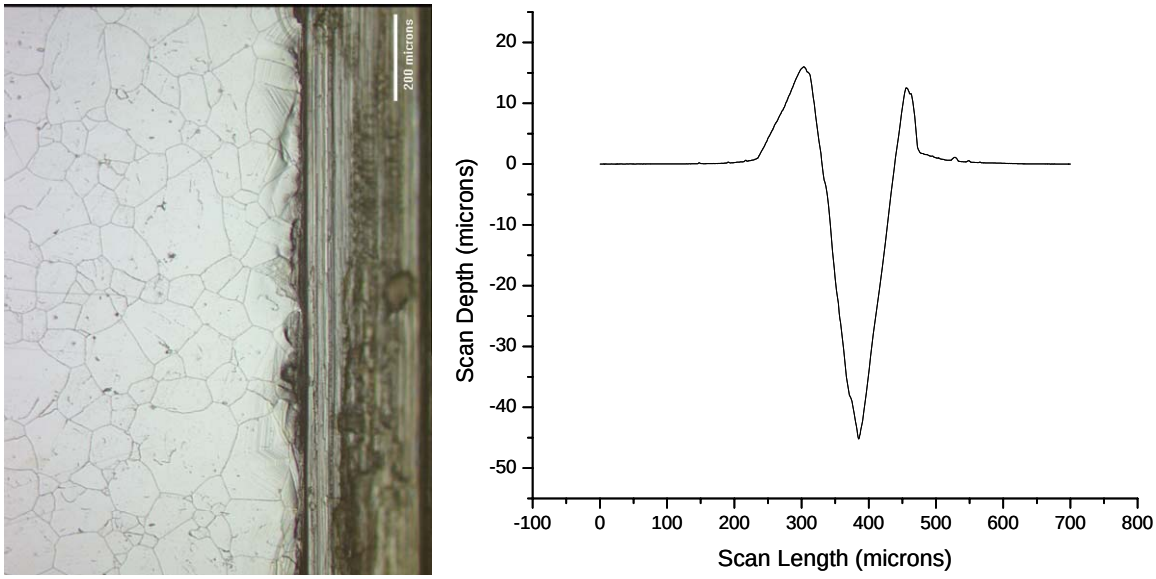

Figure 3. An optical micrograph of the 'coarse' scratch (left figure) generated on polished Alloy 600 coupon surface. The scratch is at the far right of this figure and the adjacent areas have been etched to reveal the grain structure. Slip lines emanating from the edge of the scratch can also be seen in this figure. Surface profile scan across the scratch (right figure) indicates that the scratch is approximately 100 μm wide and 40 μm deep.

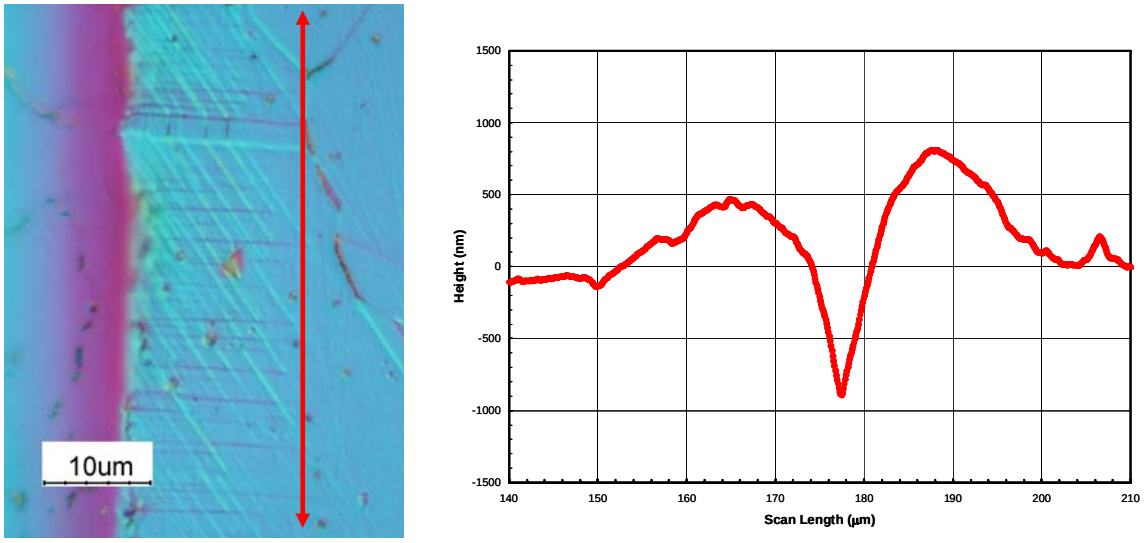

Figure 4. An optical micrograph of the 'fine' scratch (left figure) generated using a spherical diamond tipped nano indenter. The scratch is at the far left of this figure and the slip lines emanating from the edge of the scratch can be seen. The red line indicates the region up to which the slip lines extend away from the scratch across the metal surface. Surface profile scan across the scratch (right figure) indicates that the scratch is approximately 20 µm wide and 1.5 µm deep. Pile up of material at the edge of the scratch can also be seen in this figure.

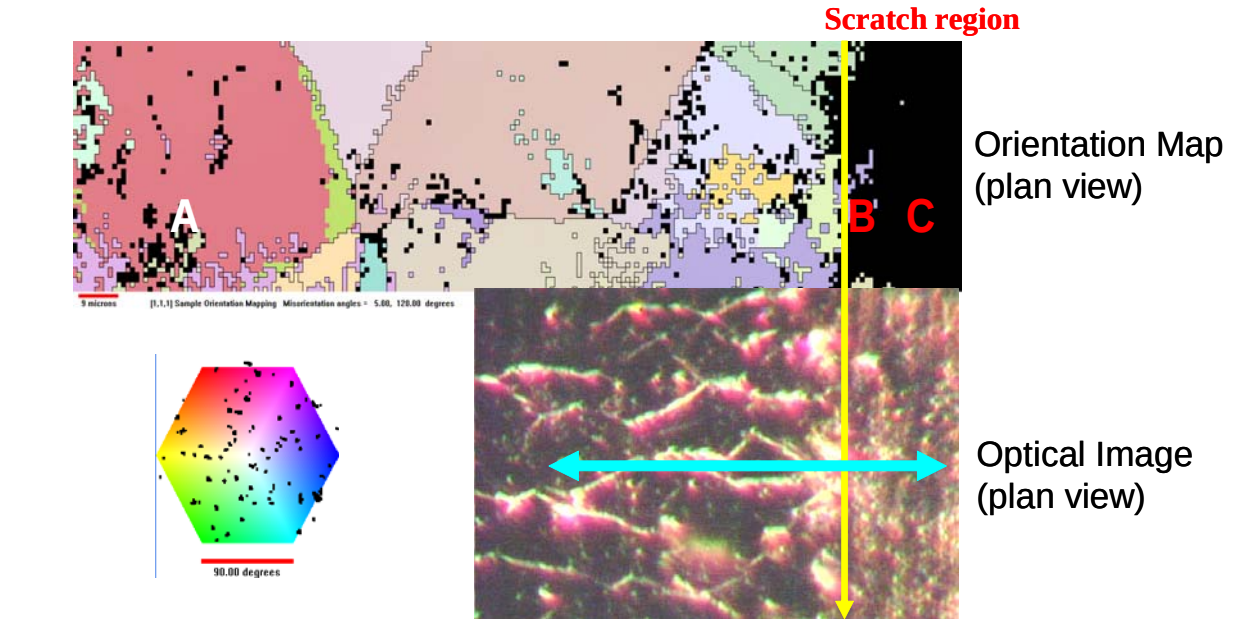

Figure 5. 2-dimensional grain orientation map for the [1,1,1] crystallographic direction within the analysis area (200 μm x 50 μm) on the coarse scratch sample. The bottom right figure is a telescopic image of the etched surface and the scratch is at the far right. The top figure presents the orientation of various grains within the area of interest. The area within the scratch did not get indexed due to the significant deformation sustained in this region. The spots A (away from scratch) , B (scratch edge) , C (scratch region) correspond to the CCD camera images of the Laue diffraction pattern presented in Figure 6.

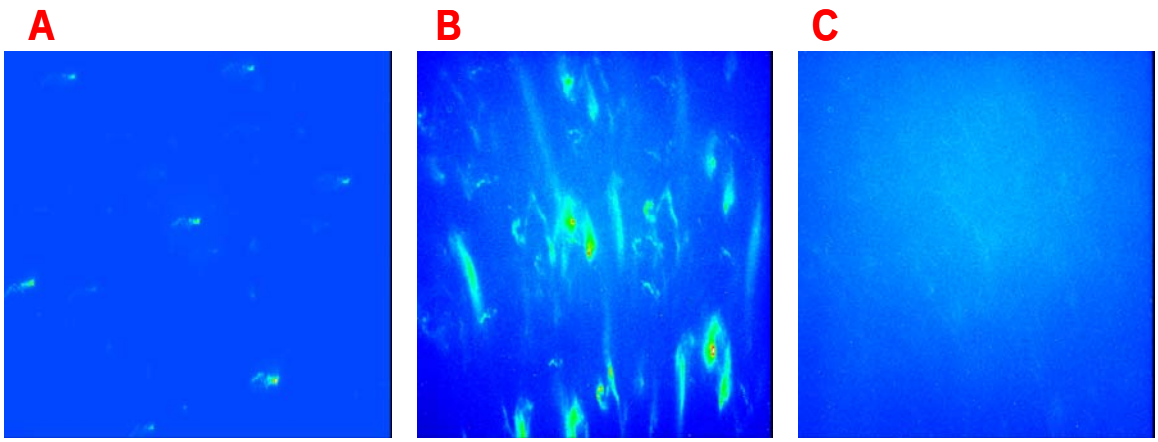

Figure 6. CCD camera images of Laue diffraction patterns from locations A, B and C shown in Figure 5. Spot C is within the scratch and the diffraction pattern appears to be diffused suggesting the presence of a nanocrystalline phase in this region. The region near the edge of the scratch (B) appears to be heavily streaked, suggesting significant plastic deformation in this region. Finally, region A (away from the scratch) exhibits moderate streaking, indicating some plastic deformation in this region.

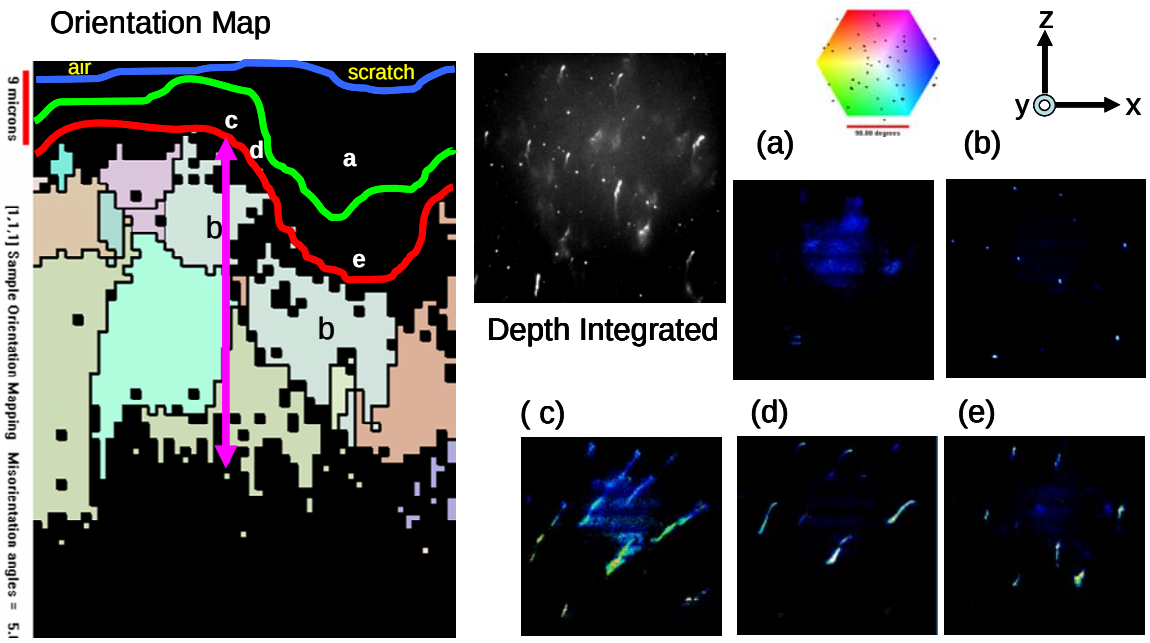

Figure 7. Laue diffraction data from the fine scratch sample. The figure on the left is the depth-resolved grain orientation map for the [1,1,1] crystallographic direction of the area analysed. The solid blue line across the top of the orientation map indicates the sample surface, above which the reconstructed CCD images were found to be devoid of any structure. CCD images from between the solid blue and green lines were found to exhibit diffuse structure (no defined Laue spots) as shown in CCD image (a), corresponding to that from position ‘a’ in the OM. The CCD image (b) from the grain labelled ‘b’ in the OM exhibits well-defined round spots. On the other hand, the CCD images (c) and (d) from positions ‘c’ and ‘d’ in the OM exhibit severe streaking towards the top right corner of the CCD image. These CCD images are believed to originate from the side of the scratch. The CCD image (e) from position ‘e’ in the OM also exhibits streaking, however, the streaking is more vertical than that seen in (c) and (d).

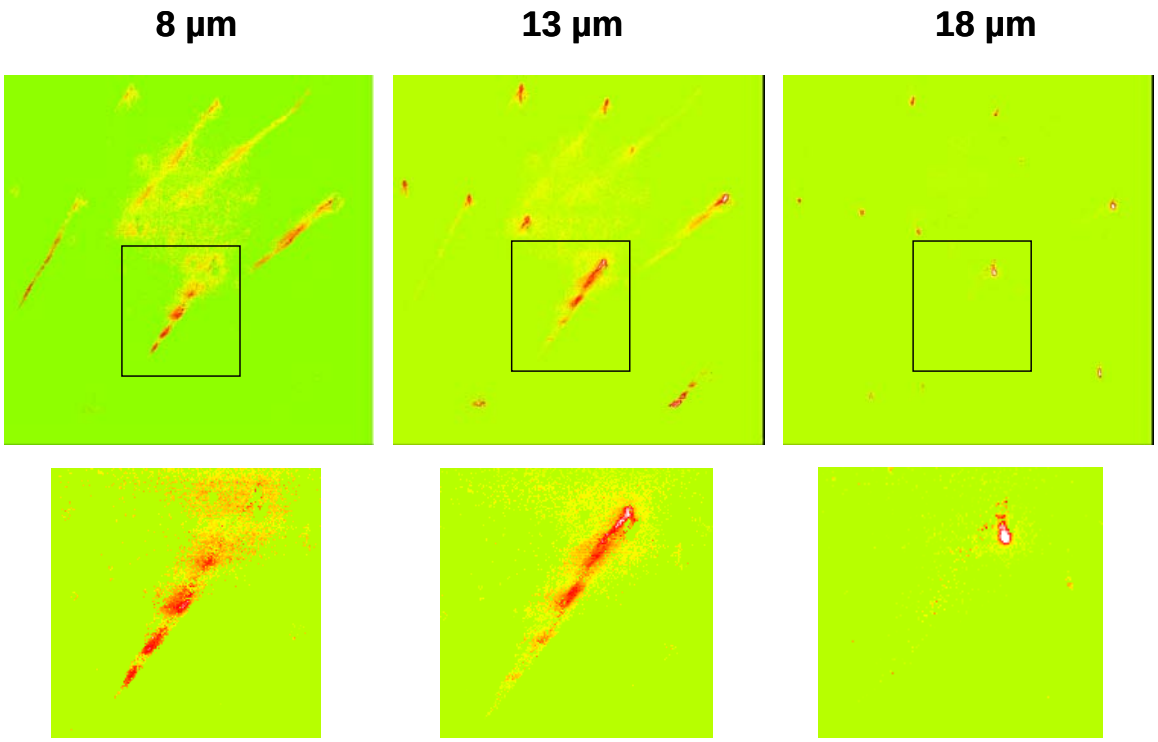

Figure 8. CCD camera images of Laue diffraction pattern collected at various depths along the purple line shown in Figure 7. The areas within the black boxes are blown up below for comparison. This figure shows the splitting of Laue spots (8 µm depth) which has been attributed to the build-up of dislocation cells in this 1 micron sample volume.

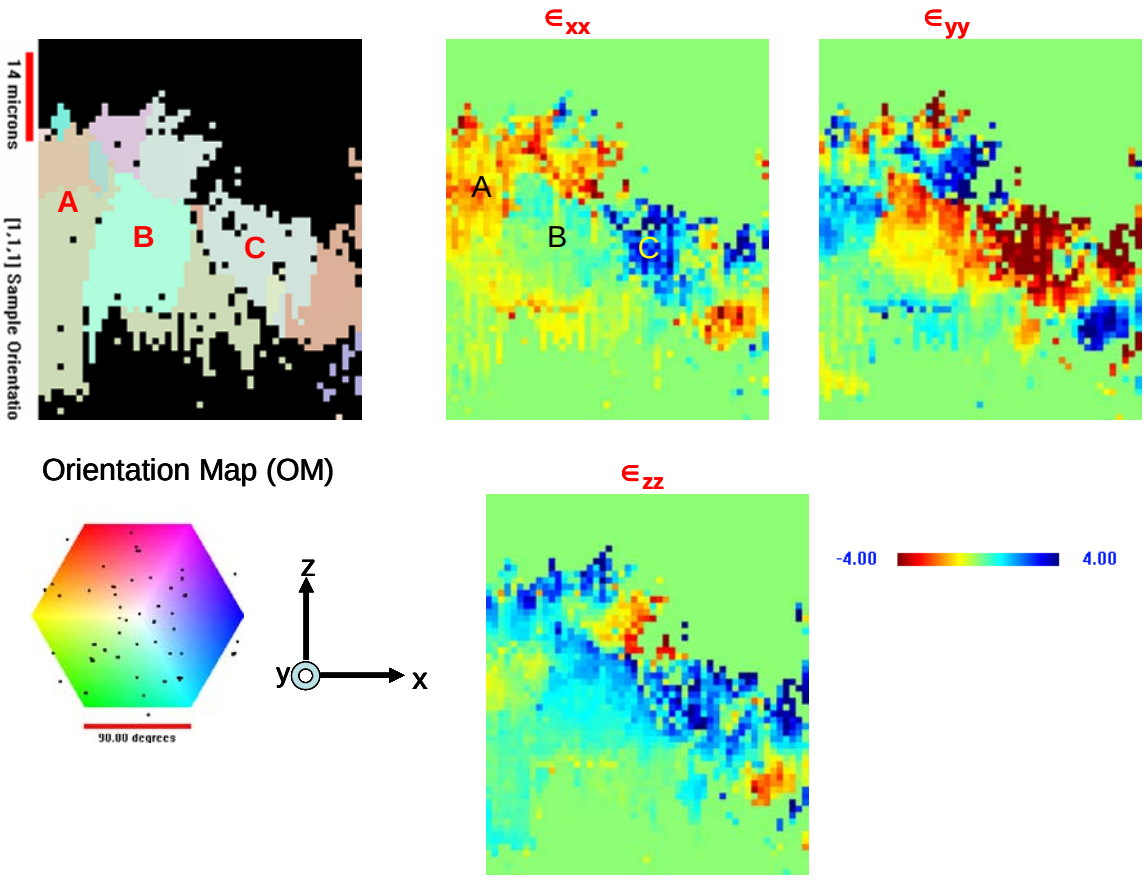

Figure 9. Deviatoric strain component maps collected from the area of interest on the fine scratch sample. The strain values are in 10^{-3} units and a thermal scale has been employed to show the distribution of tensile and compressive strains within the analysis area. Coordinates of sample orientation matrix in indexed files: y-direction is in the direction of the generated scratch, x-direction runs perpendicular to the scratch direction and the z-direction is perpendicular to the sample surface (i.e., the DAXM line scan was taken perpendicular to the scratch). The regions marked A-C in the ϵ_{xx} strain component map correspond roughly to the grain structure in the OM. The grains on either side of grain B (A and C) are in different states of strain, A being compressive and C tensile. The grains under the scratch show triaxial strain.